Available online at www.sciencedirect.com
SCIENCE DIRECT®
Journal of Solid State Chemistry 178 (2005) 1284–1291
JOURNAL OF SOLID STATE CHEMISTRY
www.elsevier.com/locate/jssc

Towards an insight on the photoluminescence of disordered $CaWO_4$ from a joint experimental and theoretical analysis

Emmanuelle Orhan[a,*], Marcos Anicete-Santos[a], Maria A.M.A Maurera[b], Fenelon M. Pontes[c], Antonio G. Souza[b], Juan Andrès[d], Armando Beltràn[d], José A. Varela[a], Paulo S Pizani[e], Carlton A. Taft[f], Elson Longo[c]

[a]*Instituto de Química, Universidade Estadual Paulista, 14801-907 Araraquara, SP, Brazil*
[b]*CCEN Departamento de Química, Universidade Federal da Paraiba, Campus I, 58059-900 João Pessoa, PB, Brazil*
[c]*Departamento de Química, Universidade Federal de São Carlos, 13565-905 São Carlos, SP, Brazil*
[d]*Departament de Ciències Experimentals, Universitat Jaume I, 12080 Castelló, Spain*
[e]*Departamento de Física, Universidade Federal de São Carlos, 13565-905 São Carlos, SP, Brazil*
[f]*Centro Brasileiro de Pesquisas Físicas, 22290-180 Rio de Janeiro, RJ, Brazil*

Received 12 November 2004; received in revised form 21 December 2004; accepted 30 December 2004

Abstract

A joint experimental and theoretical study has been carried out to rationalize for the first time the photoluminescence (PL) properties of disordered $CaWO_4$ (CWO) thin films. From the experimental side, thin films of CWO have been synthesized following a soft chemical processing, their structure has been confirmed by X-ray diffraction data and corresponding PL properties have been measured using the 488 nm line of an argon ion laser. Although we observe PL at room temperature for the crystalline thin films, the structurally disordered samples present much more intense emission. From the theoretical side, first principles quantum mechanical calculations, based on density functional theory at B3LYP level, have been employed to study the electronic structure of a crystalline (CWO-c) and asymmetric (CWO-a) periodic model. Electronic properties are analyzed in the light of the experimental results and their relevance in relation to the PL behavior of CWO is discussed. The symmetry breaking process on going from CWO-c to CWO-a creates localized electronic levels above the valence band and a negative charge transfer process takes place from threefold, WO_3, to fourfold, WO_4, tungsten coordinations. The correlation of both effects seems to be responsible for the PL of amorphous CWO.
© 2005 Elsevier Inc. All rights reserved.

Keywords: Ab initio calculations; Ceramics; Crystals; Photoluminescence; Thin layers

1. Introduction

Calcium and lead molybdates and tungstates are well known for their interesting luminescence and structural particularities and therefore have been extensively studied during the past century. For example, Kröger wrote a monograph presenting a complete summary of the luminescence properties of these and related materials [1]. Among those naturally occurring minerals, $CaWO_4$ (CWO) has been well known for a long time for its strong visible luminescence, allowing for instance to find the tungstate-rich ores in tungsten mines by using ultraviolet lamps. It was also used for 75 years in X-ray photography as screen intensifies due to its capability of absorbing X-rays and converting their energy into radiation enabling the blackening of the photographic film [2]. Nowadays the challenge is to use CWO as solid-state optoelectronic devices like lasers, optical fibers

*Corresponding author. Laboratorio Interdisciplinar de Electroquimica e Ceramica, Centro Multidisciplinar para o Desenvolvimento de Materiais Ceramicos, Universidade Federal de Sao Carlos, Via Washington Luiz, Km. 235, Caixa Postal 676, CEP: 13.565-905 Sao Carlos, Sao Paulo, Brazil. Fax: +55 16 3351 8214.
E-mail address: emmanuelle.orhan@liec.ufscar.br (E. Orhan).

0022-4596/$ - see front matter © 2005 Elsevier Inc. All rights reserved.
doi:10.1016/j.jssc.2004.12.038

components or scintillators [3–6]. CWO is also the object of interesting structural studies because it presents a great variety of phases depending on the preparation conditions [7,8].

Numerous papers report the photoluminescence (PL) behavior of crystalline $CaWO_4$. When excited by short-wavelength ultraviolet radiations (around 250 nm) at room temperature, it mainly presents a blue emission band at around 420 nm, which is commonly attributed to the WO_4 tetrahedra [9], or to self-trapped electron states [10]. A green emission band also exists at around 490 nm, whose origin is a bit controversial. It already has been attributed to WO_3 defect centers associated with oxygen vacancies [11,12] or to intrinsic transitions in the WO_4^{2-} complex [13,14]. Very little information is available on the luminescence spectra under longer wavelength excitations.

In the present paper, the PL of non-crystalline $CaWO_4$ is investigated for the first time. Visible PL at room temperature in disordered materials was first observed by Canham in porous silicon [15] and since then the study of PL in disordered or nanostructured materials has been the focus of numerous studies, mainly on titanate compounds [16–22]. We are combining laboratory experiments and high-level calculations into a synergetic strategy for understanding the PL origin in disordered $CaWO_4$. The experimental work presents measurements of broad, intense PL at room temperature in structurally disordered CWO thin films prepared by the polymeric precursor method. This process offers advantages over other synthesis techniques such as low cost, good compositional homogeneity, high purity, low processing temperatures and ability to coat large substrate areas.

The aim of the theoretical part is to investigate the electronic structure of CWO by using models representing its crystalline and disordered structures and to give an interpretation in terms of density of states (DOS) and band structure diagrams of the conditions allowing PL to occur at room temperature. This approach renders a plausible quantitative description of the behavior of CWO under laser excitation and an interesting correlation between the theoretical and experimental results. We do not aim to explain the mechanisms of PL in the CWO system but to explain why the intensity is much higher in the disordered films than in the crystalline one. The achievement of strong PL at room temperature from a compound processed by a low-cost method is indeed of primary interest for eventual application in solid-state optoelectronic devices.

2. Experimental

The $CaWO_4$ thin films studied in the present work were synthesized following a soft chemical method, the so-called polymeric precursor method [23]. Details of the processing have already been published [24]. The polymeric precursor solution was spin coated on substrates by a spinner operating at 7000 rev/min for 40 s (spin-coater KW-4B, Chemat Technology) via a syringe filter to avoid particulate contamination. The substrates were silicon-coated platinum and quartz. After spinning, the films were kept in ambient air at 423 K on a hot plate for 20 min to remove residual solvents. They were then annealed at different temperatures from 573 to 873 K for 4 h in air atmosphere.

The CWO thin films were structurally characterized by X-ray diffraction (XRD) using Cu$K\alpha$ radiation source. The diffraction patterns were recorded on a Siemens D5000 machine in a $\theta - 2\theta$ configuration using a graphite monochromator. The spectral dependence of optical absorbance for the crystalline and amorphous CWO thin films was measured in the wavelength range from 200 to 800 nm, using a Cary 5G spectrophotometer. The PL spectra of the CWO thin films were recorded with a U1000 Jobin–Yvon double monochromator coupled to a cooled GaAs photomultiplier and a conventional photon counting system. The 488 nm exciting wavelength of an argon ion laser was used, with the laser's maximum output power kept at 60 mW. A cylindrical lens was used to prevent the sample from overheating. The slit width used was 100 μm. All measurements were taken at room temperature. Atomic force microscopy (AFM) was used to obtain a 3D image reconstruction of the sample surface. These images allow for an accurate analysis of the sample surface and quantification of highly relevant parameters such as roughness and grain size. A Digital Instruments Multi-Mode Nanoscope IIIa was used.

3. Computational methods

Calculations have been carried out with the CRYSTAL98 package [25], which is based on both Density Functional (DFT) and Hartree–Fock theories. The gradient-corrected correlation functional by Lee, Yang and Parr was used, combined with the Becke 3 exchange functional, B3LYP [26,27], which has been demonstrated by Muscat et al. [28] to be suitable for calculating structural parameters and band structures for a wide variety of solid-state compounds. The basis sets used for describing O and Ca atomic centers can be found in Ref. [29] and for W in the paper by Cora et al. [30]. The k-points sampling was chosen to be 40 points within the irreducible part of the Brillouin zone. For simulating the displacement of the W2 and W4 atom (as defined in Fig. 1), we have used the atom displacement option provided with the CRYSTAL program. The XCrysDen program was used to design the DOS and the band structure diagrams [31].

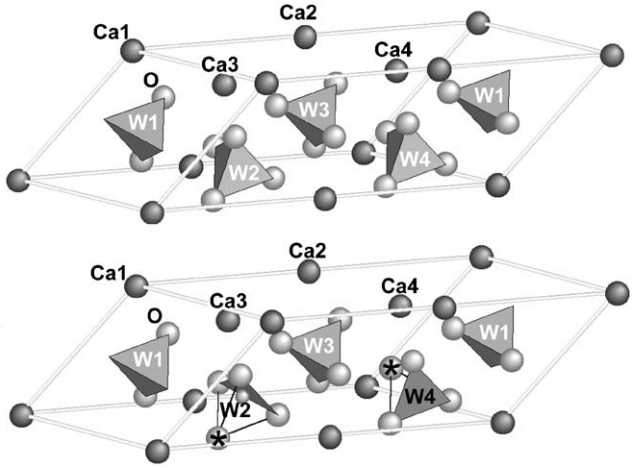

Fig. 1. CWO-c periodic model: $1 \times 1 \times 2$ supercell of the $CaWO_4$ primitive unit cell (top). CWO-a periodic model: W2 and W4 are shifted in the direction opposite to the starred oxygen atoms (bottom).

4. Crystal structure and periodic models

The scheelite $CaWO_4$ crystallizes in a tetragonal structure (space group $I4_{1/a}$, C_{4h} symmetry). Tungsten atoms are surrounded by four oxygen atoms in a tetrahedral configuration and calcium atoms are surrounded by eight oxygen atoms in a pseudo-cubic configuration. The experimental **a** and **c** parameters are, respectively, 5.2429 and 11.3737 Å [32]. The optimization of the cell parameters was not necessary as the preliminary results obtained with the experimental parameters gave an energy gap value equal to the experimental one (see Section 5). The Crystal98 code transforms the conventional cell into the primitive cell for simplifying the calculations. In this case, the primitive cell parameters are $a = b = c = 6.7885$ Å, $\alpha = \beta = 134.5687^\circ$ and $\gamma = 66.2011^\circ$. We have used a $1 \times 1 \times 2$ supercell of the primitive cell as a periodic model for representing the crystalline CWO (CWO-c). It results in 24 atoms in the supercell, see top part of Fig. 1.

Various authors attribute the green PL component of $CaWO_4$ (around 490 nm) to the existence of some WO_3 truncated tetrahedra in the crystalline scheelite [11,13,33,34]. We assume that before the complete crystallization of the film, i.e., before the heat treatment reaches 873 K, the structure is composed of a random mixture of WO_4 and WO_3 tetrahedra linked by the Ca ions. This assumption is based on our experience with titanates: XANES experimental results on the crystallization process of $SrTiO_3$ and $PbTiO_3$ [17,35] pointed out the coexistence of two types of environments for the titanium, namely, fivefold titanium coordination ($[TiO_5]$ square-base pyramid) and sixfold titanium coordination ($[TiO_6]$ octahedron), from the citrate solution to the disordered powder, when synthesized by the polymeric precursor method. This certain degree of order in structurally disordered materials was to be expected, since two or more atoms arranged close to each other in a stable configuration must necessarily have some degree of order because there always are minima of the potential energy. Furthermore, as it is well known, the details of the band structure for a periodic system are mainly determined by the potential within the unit cell rather than by the long-range periodicity. This means that any symmetry perturbation in the unit cell will have consequences on the electronic structure.

We thus created a $1 \times 1 \times 2$ supercell that will stand for the non-crystalline phases. Starting from the previous CWO-c model, the W2 and W4 atoms were shifted by 0.3 Å in the direction opposite to the starred oxygen atoms as to break the bonds (see bottom part of Fig. 1). This 0.3 Å value was chosen after tests at 0.1, 0.2, 0.4 and 0.5 Å because it was the first value allowing to see clearly the effects of bond deformation on the electronic structure and that reproduces quite well the experimental value of the band gap energy. This new periodic model will be called CWO-a, for being asymmetric. W2 and W4 are now surrounded by three oxygen atoms in their first coordination sphere.

Our aim with the use of this CWO-a model is to offer a simple scheme allowing to understand the effects of a structural deformation on the electronic structure without completely suppressing the geometry of the cell that is useful for the periodic calculations. Using the same kind of distorted model, we have successfully explained the PL of various perovskite titanates [18,19,36,37].

5. Results and discussion

Fig. 2 shows the XRD patterns of CWO thin films deposited on silicon substrate after different annealing

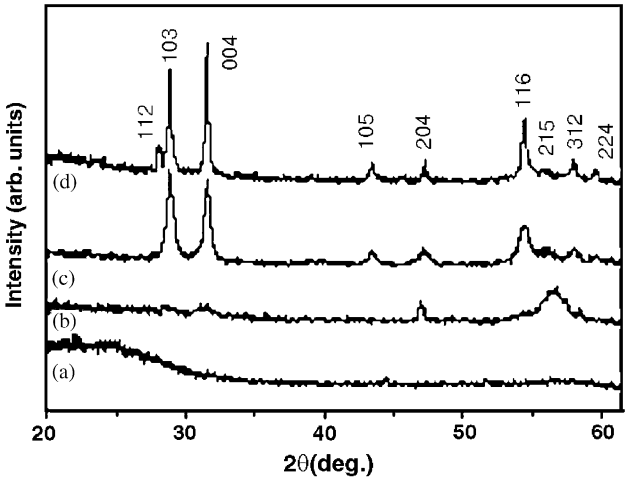

Fig. 2. XRD patterns for the thin films annealed at (a) 573 K, (b) 673 K, (c) 773 K and (d) 873 K for 4 h.

temperatures: 573, 673, 773 and 873 K. A diffuse pattern is observed for the films treated at 573 and 673 K, indicating the formation of an inorganic disordered phase after the pyrolysis process. The crystallization of the CWO scheelite phase starts at 773 K but all peaks are visible and well-defined only at 873 K. All peaks are ascribed to the tetragonal structure, matching with the JCPDS 41-1431 card.

A closer observation of the structure of two films annealed at 473 and 873 K made by AFM shows the difference between them in terms of surface morphology (see Fig. 3). The CWO thin film annealed at 423 K possesses a homogeneous surface morphology with very low roughness. There was no evidence of a granular structure. The surface morphology of the CWO changes dramatically at 873 K. At this stage of growth, coalescence of nuclei occurs, with formation of granular structures resulting in a significant increase in roughness. This result is in agreement with the XRD analysis, where at 873 K a high crystallization can be observed.

Fig. 4 shows the PL spectra, measured at room temperature, for the thin films annealed at 573, 673 and 773 K. They were excited by the 488 nm line of an argon ion laser. The profile of the emission band is typical of a multiphonon process, i.e., a system in which relaxation occurs by various paths, involving the participation of

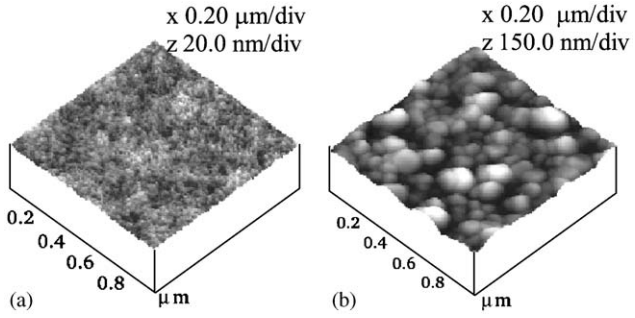

Fig. 3. AFM images of the thin films annealed at (a) 423 K and (b) 873 K.

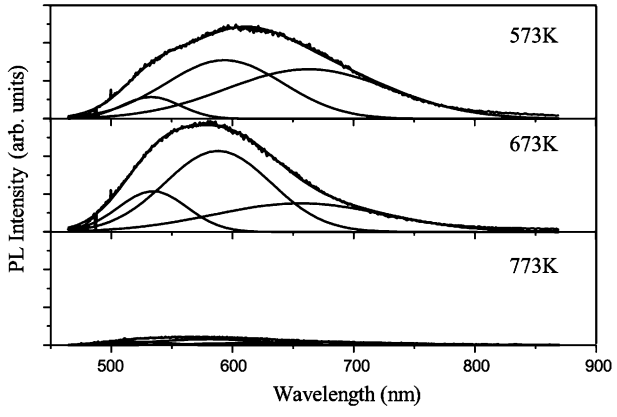

Fig. 4. PL spectra of the thin films annealed at 573, 673 and 773 K.

numerous states. The spectra general aspect is a broadband covering a large part of the visible spectra. That band can be decomposed into three components: three broadbands at approximately 530 nm (green), 580 nm (yellow) and 650 nm (red). At 673 K, the PL intensity is at its maximum, the yellow contribution being the most important. For the sample annealed at 573 K, the PL intensity decreases. From 773 K, the thin film is well crystallized and its PL becomes very weak in relation to the PL of the disordered thin films. The PL intensity is linked to the thermal treatment history of the powders, and thus to the structural disorder. The best PL emission is obtained for the structure that is neither completely disordered (573 K) nor completely ordered (773 K). The three components of the PL emission bands are probably linked to specific atomic arrangements. The structural transformations occurring from disordered to ordered phases start from the early stage of the polyesterification of the citrate solution containing the tungsten and calcium ions. The tungsten, which is the lattice former, tends ideally to bond with four oxygen atoms, but before it reaches this ideal configuration, there exist various coordination numbers for W in the structure. When the crystallization is reached, only WO_4 clusters exist and the PL vanishes, showing that a complete order is not suitable for a good PL emission. Before the crystallization, the structure is a mixture of WO_x clusters ($x =$ mostly 3 and 4) intercalated by Ca atoms. The higher the heat treatment temperature, the more frequent the WO_4 conformation and the more ordered the structure. The PL spectra show that a complete disorder is not favorable for a high PL emission, as the spectrum of the 673 K sample is much higher than the one of the 573 K sample.

It has to be underlined that our excitation energy (2.54 eV) is smaller than that corresponding to the 420 nm emission wavelength (blue) frequently attributed to the regular tungstate group, and thus that it cannot be observed. To our knowledge, no data of CWO powders or thin films excited with a 488 line are available.

The aforementioned experimental results strongly indicate that the PL of CWO is very sensitive to its structure and that relatively weak variations in the atomic arrangements can induce significant changes in the emission spectra. In Fig. 5, the spectral dependence of the absorbance of two thin films is presented; the first one was annealed at 673 K and the second one, crystalline, at 873 K. The crystalline thin film presents well-defined interband transition with quasivertical absorption front, typical of semiconductor crystalline materials. The non-crystalline thin film exhibits a smoother slope with a tail at low energies, suggesting the presence of localized states inside the band gap of the film. The optical gaps obtained by extrapolation of the linear curve regions according to the Wood and

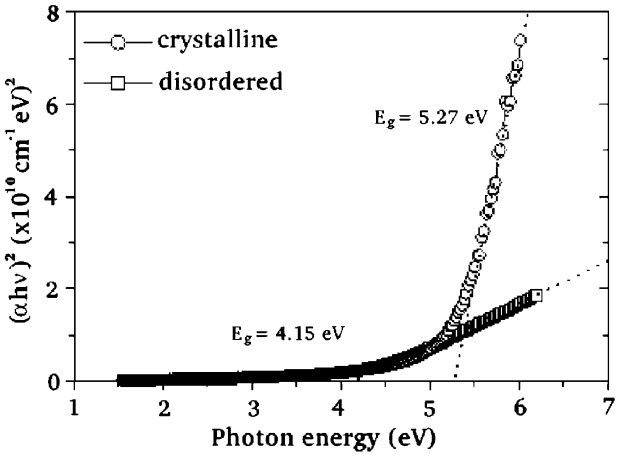

Fig. 5. Spectral dependence of the absorbance for the thin films annealed at 623 K (squared symbols) and at 873 K (round symbols).

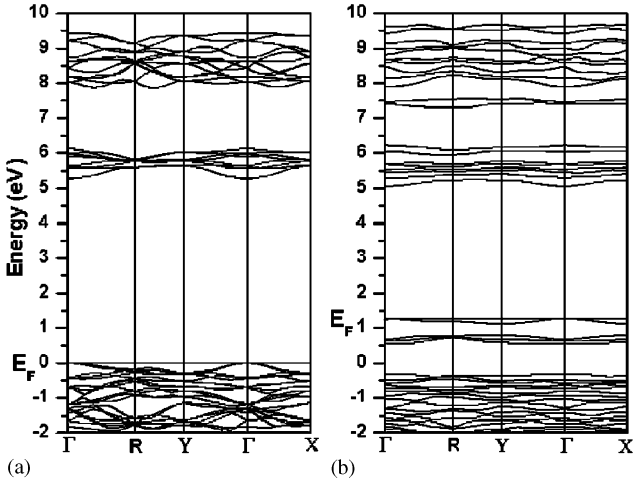

Fig. 6. Band structure for the CWO-c (a) and CWO-a (b) models. In both cases, the zero corresponds to the Fermi energy of the CWO-c structure.

Tauc method are 5.27 eV for the crystalline thin film and 4.15 eV for the structurally disordered one [38]. The presence of the optical tail may be associated with defect states promoted by the disordered structure of $CaWO_4$ thin film before it crystallizes. As the band gap energy is much higher than the excitation energy that is used for collecting the PL spectra (2.54 eV), the mechanism giving rise to PL is not a band to band process. It must be linked to the defect states. Montoncello et al. [39] pointed out that PL often highlights features that absorption measurements would rarely define, like the properties of the energy levels lying within the band gap of a material.

The absorbance measurements, associated with the PL characterization of amorphous $CaWO_4$ thin films, suggest a non-uniform band gap structure with a tail of localized states and mobile edges. As explained by Blasse [2], the PL arises from a radiative return to the ground state, a phenomenon that is in concurrence with the non-radiative return to the ground state where the energy of the excited state is used to excite the vibrations of the host lattice, i.e., to heat the lattice. The radiative emission process occurs more easily if it exists in the structure-trapped holes or trapped electrons. In order to evidence their presence in our structurally disordered thin films, we performed a detailed theoretical study of the electronic structure in two models: a tetragonal CWO-c, and a disordered (asymmetric) CWO-a. The first model represents the crystalline CWO thin film and the second one a thin film whose crystallization is incomplete. To analyze the differences in the electronic structure, it is convenient to make reference to quantities such as the band gap, the projected DOS or the charge density maps, which may be compared to each other independent of the crystalline space group.

Fig. 6a shows the calculated band structure of bulk CWO-c. The gap is direct at Γ and its value is 5.27 eV, equal to the experimental value deduced from the optical absorption edge (see Fig. 5). Zhang et al. calculated a 4.09 eV direct band gap using a linearized augmented plane wave DFT method, well known to underestimate the energy gap value [40]. The calculated band structure of bulk CWO-a is represented in Fig. 6b. The gap is also direct at Γ and its value is 3.78 eV. The calculated gap can be compared with the optical gap of the thin film annealed at 573 K, that is 4.15 eV (see Fig. 5). These results show that our data are consistent with the interpretation that the exponential optical absorption edge and the optical band gap are controlled by the degree of disorder, structural and thermal, in the lattice of CWO.

To analyze what new levels were created inside the gap of the crystalline structure, an energy diagram was plotted. In Fig. 7, the main contributions for each band (taken at Γ point) are schematically represented as energy levels, for one regular, symmetric model and for one model containing shifted tungsten, as in the CWO-c and CWO-a models. The two models are based on only one primitive CWO unit cell, as shown at the bottom part of Fig. 7. We extracted the states belonging to the shifted tungsten atom, W*, and to the four oxygen atoms forming its coordination sphere for simplifying a global view of what happens with the increase in the W*–O* bond length. In Fig. 7a, the splitting of the W*(5*d*) levels is typical of tetrahedral coordination, t_2 and *e*. By elongating the W*–O* bond of 0.3 Å, new states located "in" the band gap of the crystalline CWO were created, in accordance with the absorbance tail observed for CWO thin film before crystallization (see Fig. 5). It is clear from Fig. 7b that the new states created above the valence band of the crystalline CWO are due to the 2*p* orbitals of the starred oxygen, i.e., the

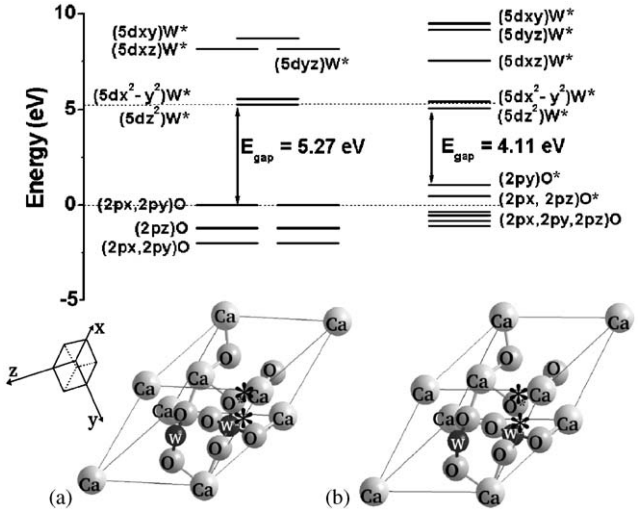

Fig. 7. Representation of the main contributions of W* and O* atoms to the crystal orbitals taken at Γ point for one regular primitive unit cell (a) and for one primitive unit cell where W* has been shifted away from O* by 0.3 Å (b).

oxygen whose bond with W* was broken. The levels appearing below the conduction band are of W*$5dz^2$ character. Although not shown in Fig. 7, the Ca contribution to the valence band is also shifted toward the highest energies. The W*–Ca distance is longer and the interaction weaker. This simple scheme offers a supplementary interpretation of the presence of various bands in the PL spectra of the CWO thin films. The highest energy bands, green and yellow, may be the illustration of a radiative decay occurring from the W* (5*d*) orbitals to the O (2*p*) while the decay corresponding to the red band would be from W* (5*d*) to O* (2*p*).

The calculated total and atom-resolved DOS of CWO-c and CWO-a models are shown, respectively, on the top and the bottom parts of Fig. 8. The energy window ranges from −7 to 10 eV. The zero is taken at the Fermi level of CWO-c in both cases. For CWO-c, the upper VB is mainly made of the O (2*p*) states and equivalently distributed on each oxygen. For CWO-a too, the upper VB is predominately made of the O (2*p*) states but the states above the 0 energy are mostly of O* characters, the two oxygen atoms that lose the connection with W2 and W4. The CB is clearly made of the W (5*d*) states in both cases. As already noted in Fig. 7b, the new states created below the CB of the CWO-c are due to the $5dz^2$ orbitals of the shifted tungsten atoms, W2 and W4.

A comparison of the Mulliken charge distribution in both periodic models reveals that the breaking of W–O bonds does not lead to charge transfer from one atom to another, like widely admitted [2], but from cluster to cluster. The maximal atomic charge changes occur for the two tungsten ions that are dislocated, W2 and W4, and for the two oxygen atoms from which they are

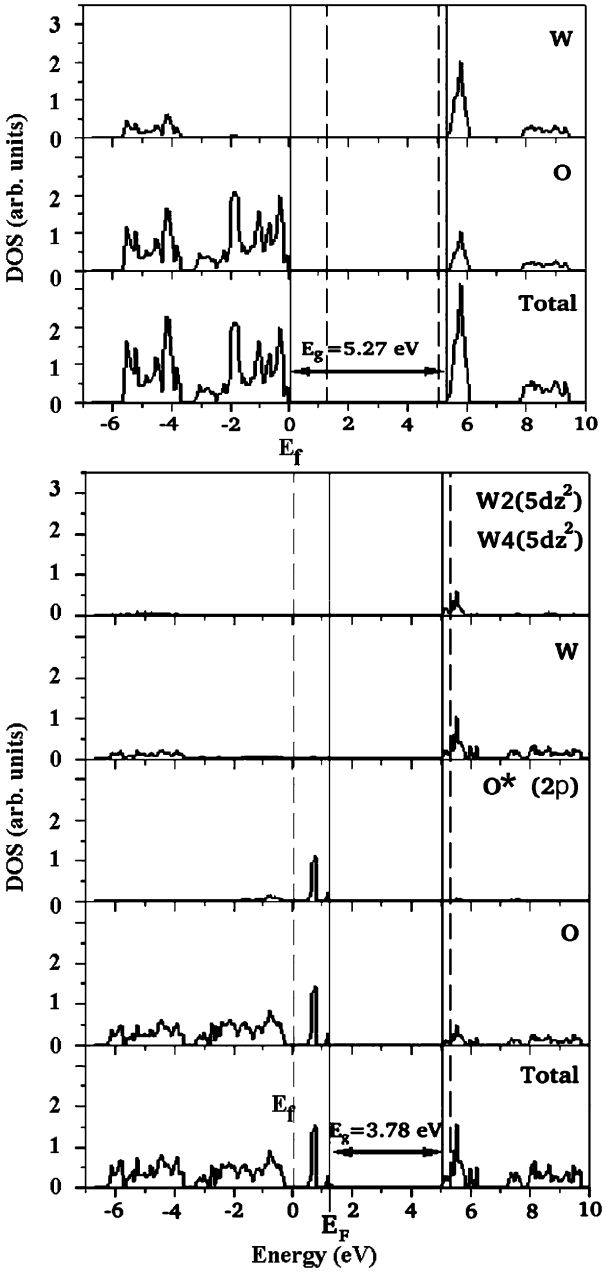

Fig. 8. Total, atom- and atomic orbital-projected DOS for the CWO-c model (top) and for the CWO-a model (bottom).

moved away, O*. Those changes are, respectively, +0.075*e* and −0.081*e*, very weak with respect to the variations in the cluster charges that are presented in Table 1. In the $CaWO_4$ structure, the tungstate tetrahedra are not only isolated from each other in the crystal-chemical sense, i.e., they do not share oxygen ions, but also electronically [41]. The untouched WO_4 clusters keep the same charge along the structural deformation, while the CaO_8 clusters neighboring the deformed WO_4 are strongly perturbed (+0.22*e*). The charge variation from the deformed WO_4 to WO_3 clusters is a loss of 0.43*e*.

Table 1
Charge variations for each individual cluster of the structure before and after deformation

Cluster designation	Charge of the CWO-c clusters (e)	Charge of the CWO-a clusters (e)	Charge difference (e)
$Ca1O_8$	−1.64	−2.04	+0.40
$Ca2O_8$	−1.64	−1.68	+0.02
$Ca3O_8$	−1.64	−1.86	+0.22
$Ca4O_8$	−1.64	−1.86	+0.22
$W3O_4$	1.64	1.65	−0.01
$W1O_4$	1.64	1.65	−0.01
$W2O_x$[a]	1.64	2.07	−0.43
$W4O_x$[a]	1.64	2.07	−0.43

[a] x= 4 for CWO-c and $x = 3$ for CWO-a.

A charge gradient thus exists in the structure before excitation. This gradient, together with the localized states appearing in the band gap, allows the electrons to self-trap, in accordance with the study of Zhang et al. [40] who reported that excitons self-trap before emitting luminescence photons in CWO. Because of the significant local lattice distortion that accompanies self-trapping, the states giving rise to luminescence can be described as molecular orbitals of the single distorted atomic group on which the extra charge localizes, that is to say WO_3 clusters. This phenomenon episodically occurs in the crystalline structure, leading to the well-known visible PL of CWO, but is far more frequent in the disordered thin film, because all the conditions favorable to self-trapping are present.

6. Conclusions

Thin films of CWO have been synthesized following a soft chemical low-cost processing and new PL behavior has been evidenced. For the first time, the intense room-temperature visible PL of non-crystalline CWO thin films is discussed. In accordance with the measured optical tails, the existence of localized levels in the band gap of the crystalline compound when it is deformed has been proven. The main character of those localized levels is 2p of the oxygen atoms losing the connection with the tungsten for the states appearing above the valence band and 5dz2 of these particular tungsten for the states appearing below the conduction band. These results show that the chosen theoretical models are consistent with the experimental data and with the interpretation that the exponential optical absorption edge and the optical band gap are controlled by the degree of disorder, structural and thermal, in the lattice of CWO system. Moreover, a charge gradient has been observed in the deformed structure, due to the charge differences between the clusters. The coexistence of localized levels and of a charge gradient creates favorable conditions for the self-trapping of excitons before emitting luminescence photons.

Acknowledgment

This work was partially supported by the Brazilian research-financing institutions: Fundação de Amparo à Pesquisa do Estado de São Paulo—FAPESP/CEPID, by the Conselho Nacional de Desenvolvimento Científico e Tecnológico—CNPq/PRONEX and by the Programa de colaboración hispano brasileño no. PHB2001-0040.

References

[1] F.A. Kröger, Some Aspects of the Luminescence of Solids, Elsevier, Amsterdam, 1948.
[2] G. Blasse, B.C. Grabmaier, Luminescent Materials, Springer, Berlin, Heildelberg, 1994.
[3] M. Nikl, P. Bohacek, N. Mihokova, N. Solovieva, A. Vedda, M. Martini, G.P. Pazzi, P. Fabeni, M. Kobayashi, M. Ishii, J. Appl. Phys. 91 (2002) 5041.
[4] M. Nikl, P. Bohacek, E. Mihokova, M. Kobayashi, M. Ishii, Y. Usuki, V. Babin, A. Stolovich, S. Zazubovich, M. Bacci, J. Lumin. 87 (9) (2000) 1136.
[5] M. Kobayashi, M. Ishii, Y. Usuki, H. Yahagi, Nucl. Instrum. Methods Phys. Res. A 333 (1993) 429.
[6] M. Nikl, Phys. Stat. Sol. (a) 178 (2000) 595.
[7] D. Errandonea, M. Somayazulu, D. Haüsermann, Phys. Stat. Sol. (b) 235 (2003) 162.
[8] D. Errandonea, F.J. Manjón, M. Somayazulu, D. Haüsermann, J. Solid State Chem. 177 (2004) 1087.
[9] W. Van Loo, Phys Stat. Sol. (a) 28 (1975) 227.
[10] V. Pankratov, D. Millers, L. Grigorjeva, S. Chernov, Phys. Stat. Sol. (b) 225 (2) (1980) 9.
[11] J.A. Groenink, G. Blasse, J. Solid State Chem. 32 (1) (1980) 9.
[12] B.M. Sinel'nikov, E.V. Sokolenko, E.G. Zvekova, Inorg. Mater. 32 (1996) 6.
[13] Z. Lou, M. Cocivera, Mater. Res. Bull. 37 (2002) 1573.
[14] M.J. Treadaway, R.C. Powell, J. Chem. Phys. 61 (10) (1974) 4003.
[15] L.T. Canham, Appl. Phys. Lett. 57 (1990) 1046.
[16] F.M. Pontes, C.D. Pinheiro, E. Longo, E.R. Leite, S.R. de Lazaro, J.A. Varela, P.S. Pizani, T.M. Boschi, F. Lanciotti Jr., Mater. Chem. Phys. 78 (1) (2003) 227.
[17] F.M. Pontes, E. Longo, E.R. Leite, E.J.H. Lee, J.A. Varela, P.S. Pizani, C.E. M Campos, F. Lanciotti Jr, V. Mastellaro, C.D. Pinheiro, Mater. Chem. Phys. 77 (2) (2003) 598.
[18] E. Longo, E. Orhan, F.M. Pontes, C.D. Pinheiro, E.R. Leite, J.A. Varela, P.S. Pizani, T.M. Boschi, F. Lanciotti Jr, A. Beltrán, J. Andrés, Phys. Rev. B 69 (2004) 125115.
[19] E. Orhan, F.M. Pontes, M.A. Santos, E.R. Leite, A. Beltrán, J. Andrés, T.M. Boschi, P.S. Pizani, J.A. Varela, C.A. Taft, E. Longo, J. Phys. Chem. B 108 (2004) 9221.
[20] H. Pinto, A. Stashans, Phys. Rev. B 65 (2002) 134304.
[21] E. Heifets, R.I. Eglitis, E.A. Kotomin, J. Maier, G. Borstel, Phys. Rev. B 64 (2001) 235417.
[22] Ph. Ghosez, J.-P. Michenaud, X. Gonze, Phys. Rev. B 58 (1998) 6224.
[23] F.M. Pontes, E.R. Leite, D.S.L. Pontes, E. Longo, E.M.S. Santos, S. Mergulhao, P. Pizani, F. Lanciotti, T.M. Boschi, J.A. Varela, J. Appl. Phys. 91 (2002) 5972.

[24] F.M. Pontes, M.A.M.A. Maurera, A.G. Souza, E. Longo, E.R. Leite, R. Magnani, M.A.C. Machado, P.S. Pizani, J.A. Varela, J. Eur. Ceram. Soc. 23 (2002) 3001.
[25] V.R. Saunders, R. Dovesi, C. Roetti, M. Causa, N.M. Harrison, R. Orlando, C.M. Zircovich-Wilson, CRYSTAL98 User's Manual, University of Torino, Torino, Italy, 1998.
[26] C. Lee, W. Yang, R.G. Parr, Phys. Rev. B 37 (1988) 785.
[27] A.D. Becke, J. Chem. Phys. 98 (1993) 5648.
[28] J. Muscat, A. Wander, N.M. Harrison, Chem. Phys. Lett. 42 (2001) 397.
[29] available at http://www.chimifm.unito.it/teorica/crystal/crystal.html.
[30] F. Cora, A. Patel, N.M. Harrison, R. Dovesi, C.R.A. Catlow, J. Am. Chem. Soc. 118 (1996) 12174.
[31] A. Kokalj, J. Mol. Graph. 17 (1999) 176.
[32] R.M. Hazen, L.M. Finger, J.W.E. Mariathasan, J. Phys. Chem. Solids 46 (1985) 253.
[33] M. Nikl, P. Strakova, K. Nitsch, V. Petricek, V. Mucka, O. Jarolimek, J. Novak, P. Fabeni, Chem. Phys. Lett. 291 (1998) 300.
[34] M. Martini, G. Spinolo, A. Vedda, M. Nikl, K. Nitsch, V. Hamplova, P. Fabeni, G.P. Pazzi, I. Dafinei, P. Lecoq, Chem. Phys. Lett. 260 (1996) 418.
[35] E.R. Leite, F.M. Pontes, E.C. Paris, C.A. Paskocimas, E.J.H. Lee, E. Longo, P.S. Pizani, J.A. Varela, V. Mastelaro, Adv. Mater. Opt. Electron. 10 (6) (2000) 235.
[36] E. Orhan, F.M. Pontes, C.D. Pinheiro, E.R. Leite, T.M. Boschi, P.S. Pizani, A. Beltràn, J. Andrès, J.A. Varela, E. Longo, J. Solid State Chem. 177 (2004) 3979.
[37] M.S. Silva, M. Cilence, E. Orhan, M.S. Góes, M.A.C. Machado, L.P.S. Santos, C.O. Paiva-Santos, E. Longo, J.A. Varela, M.A. Zaghete, P.S. Pizani, J. Lumin., 2004, in press.
[38] D.L. Wood, J. Tauc, Phys. Rev. B 5 (1972) 3144.
[39] F. Montoncello, M.C. Carotta, B. Cavicchi, M. Ferroni, A. Giberti, V. Guidi, C. Malagu, G. Martinelli, F. Meinardi, J. Appl. Phys. 94 (3) (2003) 1501.
[40] Y. Zhang, N.A.W. Holzwarth, R.T. Williams, Phys. Rev. B 57 (1998) 12738.
[41] A.M. Van de Craats, G.J. Dirksen, G. Blasse, J. Solid State Chem. 118 (1995) 337.